Indian Geotechnical Journal, 30 (3), 2000

Vertical Displacement Interaction between Soil and Reinforcement Strip

N. Kumar Pitchumani* and M.R. Madhav†

Introduction

Horizontal reinforcements in the form of strips, sheets, grids and cells are routinely used in many reinforced earth structures. Sheet reinforcements used in highway construction help in reducing the required thickness of the subgrade. Strips, as well as sheets are used under footings to increase the bearing capacity of the soil-foundation system and to bring about a reduction in surface settlements. A number of model studies (Fragaszy and Lawton, 1984; Guido et al., 1985; Huang and Tatsuoka, 1988) and field studies (Miura et al., 1985; Jones and Dawson, 1990) establish the improvement in foundation response and bearing capacity due to reinforcement of soil. Few analytical (Giroud and Noiray, 1981; Houlsby and Jewell, 1990) and finite element solutions (Brown and Poulos, 1981; Floss and Gold, 1990) are also available. Models consisting of Pasternak shear layers, Winkler type subgrade and a rough membrane have been proposed (Madhav and Poorooshasb, 1988; Sellmeijer, 1990). Most of the studies deal with the increase in bearing capacity of reinforced foundation beds. However, settlements often govern the design. Hence, it is essential that the reductions in surface settlements due to embedded reinforcements be estimated. The present study proposes a method to predict the reduction in surface settlements due to strip form of reinforcements placed beneath a rectangular loaded area. The elastic continuum approach is adopted to solve the problem.

---

* Asst. Professor, Department of Civil Engineering, Indian Institute of Technology, Chennai – 600036, India.

† Professor, Department of Civil Engineering, Indian Institute of Technology, Kanpur – 208016, India.

Problem Definition

A strip of size, $2L_r \times 2B_r$, is placed at a depth, U_0, centrally below a rectangular area of size, $2L_f \times 2B_f$, transmitting a uniform load of intensity, q (Fig. 1). The width of the strip, $2B_r$ is relatively small ($0.1B_f$) and thickness, t_r, negligible. The surface load causes vertical and lateral displacements of points in the soil. A rigid reinforcement strip will undergo a uniform rigid body vertical displacement as shown by the full line in Fig. 2 while a deformable strip will deform as shown by the dotted curve. As a result, normal stresses are developed along the soil-strip interface. These stresses are symmetric about the vertical axis due to symmetry of the loading and geometry.

The net interfacial normal stresses considered represent the difference between the mobilised normal stresses on the top and bottom faces of the strip. Owing to the rigidity of the strip these normal stresses act upward near the centre and downward at the edges of the strip. If the strip is rigid then the strip undergoes uniform displacement resulting from this distribution of normal stresses. The net result of these mobilised stresses is to push the soil on the surface upward with a maximum value near the centre of the loaded area. Consequently, there is a reduction in settlement of points along the surface. Thus the reinforcing strip helps in reducing foundation settlements.

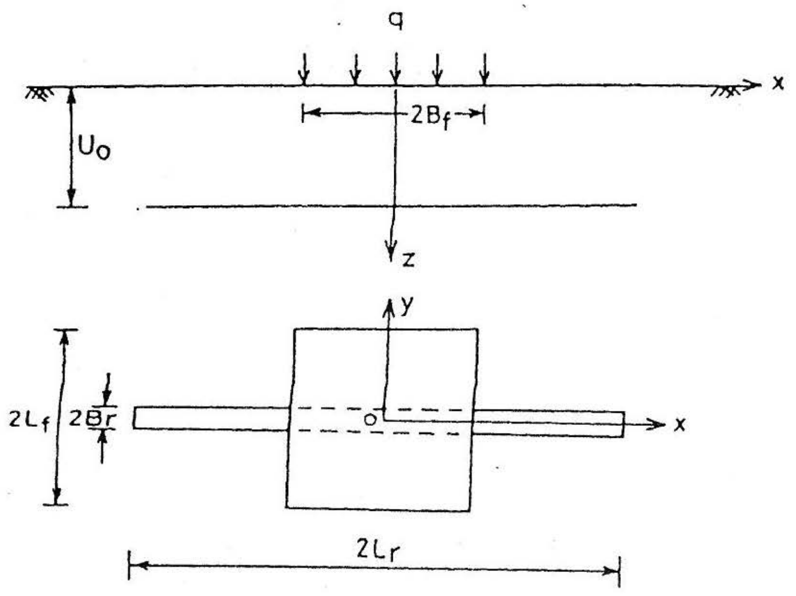

FIGURE 1 : Definition Sketch

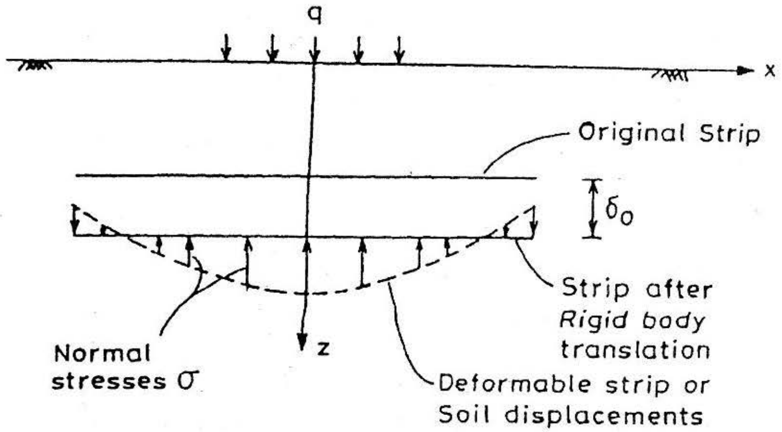

FIGURE 2 : Strip Deformation

Formulation

The elastic continuum approach is resorted to study the soil-reinforcement interaction. The soil is assumed to be homogeneous, isotropic, linearly elastic and semi-infinite in nature. Due to symmetry only half the strip is considered which is divided into N elements and over each element, the normal stress is assumed to be uniform. The vertical displacements are evaluated at the centre of each element, which is designated as a node.

The vertical displacement, ρ_{zi}^{f} of node i, along the reinforcement, due to the uniform surface load q, is obtained by integrating the Boussinesq's equation for vertical displacements due to a point load on the surface, over the loaded area as

$$\rho_{zi}^{f} = \int_{-B_f}^{B_f} \int_{-L_f}^{L_f} \frac{q(1-\nu_s)}{2\pi E_s R} \left\{ 2(1-\nu_s) + \frac{U_0^2}{R^2} \right\} dA \tag{1}$$

where $R = \sqrt{r^2 + U_0^2}$,

r = radial distance of node i, from the elemental area dA on the surface (Fig. 3),

U_0 = depth of node i, from the elemental area dA on the surface (Fig. 3),

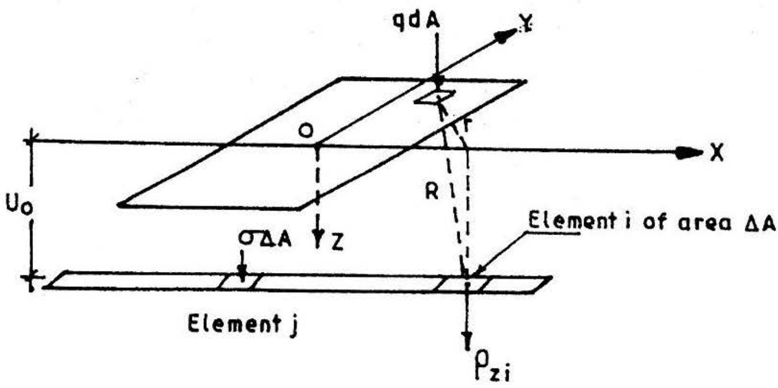

FIGURE 3 : Determination of Vertical Displacement along Strip

E_s = modulus of deformation of the soil treated as a continuum, and

ν_s = Poisson's ratio of the soil treated as a continuum

The integration is performed numerically. For this purpose, the width of the loaded area is divided into 'n_b' elements and the length into 'n_l' elements. The vertical displacement of the i^{th} node along the reinforcement is then expressed as

$$\rho_{zi}^{f} = \sum_{i_f=1}^{n_b}\sum_{j_f=1}^{n_l} \frac{q(1+\nu_s)}{2\pi E_s R}\left\{2(1-\nu_s)+\frac{U_0^2}{R^2}\right\} dA \tag{2}$$

where $R = \sqrt{r^2 + U_0^2}$,

$r = \sqrt{x^2 + y^2}$,

x and y = cartesian co-ordinates of node i,

U_0 = depth of placement of the strip, and

dA = elemental area.

Non-dimensionalising all length parameters with half-width B_f, of the loaded area, Eqn. 2 is expressed as

$$\rho_{zi}^{f} = \frac{B_f}{E_s} I_i^f q \tag{3}$$

where I_i^f is a dimensionless influence coefficient that depends on the aspect ratio, L_f/B_f of the loaded area, depth U_0/B_f of the strip, Poisson's ratio of the soil and the location of node i.

The vector of vertical displacements of all the nodes along the half-length of the strip is obtained by evaluating Eqn. 3 for all N nodes as

$$\{\rho_z^f\} = \frac{B_f}{E_s}\{I^f\}q \tag{4}$$

where the vectors $\{\rho_z^f\}$ *and* $\{i^f\}$ *are of size N.*

The vertical displacement, ρ_{zij}^{rl}, at node i, along the strip due to normal stress, σ_j, acting on element j along the strip is computed using Mindlin's equation for displacements due to a vertical force acting beneath the surface of a semi-infinite medium as

$$\rho_{zij}^{rl} = \frac{\sigma_j(1+\nu_s)\Delta A}{8\pi E_s(1-\nu_s)}(D) \tag{5}$$

where

$$D = \frac{(3-4\nu_s)}{R_1} + \frac{\left[8(1-\nu_s)^2-(3-4\nu_s)\right]}{R_2} + \frac{(z-c)^2}{R_1^3} + \frac{\left[(3-4\nu_s)\{(z+c)^2-2cz\}\right]}{R_2^3} + \frac{6cz(z+c)^2}{R_2^5}$$

$$R_1 = \sqrt{x^2+y^2+(z-c)^2}$$

$$R_2 = \sqrt{x^2+y^2+(z+c)^2}$$

x and y = horizontal distances of node i with respect to the elemental area, ΔA of the j^{th} element, and

$c = U_0 = z$.

Eqn. 5 is evaluated numerically as

$$\rho_{zxij}^{rl} = \frac{B_f}{E_s} I_{ij}^{rl}\sigma_j \tag{6}$$

where I_{ij}^{rl} is a dimensionless influence coefficient that depends on the parameters L_r/B_f and ν_s and locations of elements i and j. For every element j, there exists its image j′, normal stress on which is the same as that acting on element j. The influence of the stress acting on element j′ on the vertical displacement of node i is

$$\rho^{r2}_{zxij} = \frac{B_f}{E_s} I^{r2}_{ij} \sigma_j \tag{7}$$

where I^{r2}_{ij} is a displacement influence coefficient for the influence of the stress on element j′, on the vertical displacement of node i.

The vertical stress, σ_j, on element j and j′ act in the same direction. Combining Eqns. 6 and 7 the vertical displacement of node i due to normal stresses on all the N elements is

$$\rho^{r}_{zi} = \sum_{j=1}^{N} \frac{B_f}{E_s}\left(I^{r1}_{ij} + I^{r2}_{ij}\right)\sigma_j \tag{8}$$

The vector of vertical displacements, $\{\rho^r_z\}$, of all N nodes is expressed as

$$\{\rho^r_z\} = \frac{B_f}{E_s}[I^r]\{\sigma\} \tag{9}$$

where vectors $\{\rho^r_z\}$ and $\{\sigma\}$ are of size N and is a square matrix of size N and whose elements, $I^r_{ij} = I^{r1}_{ij} + I^{r2}_{ij}$

The net soil displacement vector, $\{\rho^s_z\}$ is obtained from the difference *of Eqn. 4 and Eqn. 9 expressed as*

$$\{\rho^s_z\} = \{\rho^f_z\} - \{\rho^r_z\} \tag{10}$$

Rigid Strip

If the strip is rigid, it undergoes uniform translation, δ_0 as shown in Fig. 2 in the vertical direction. Hence the net soil displacement equals the rigid body displacement of the strip, δ_0, i.e.

$$\{\rho^f_z\} - \{\rho^r_z\} = \{\delta_0\} = \delta_0\{1\} \tag{11}$$

Combining Eqns. 4, 9 and 11, one obtains

$$\left[I^{r}\right]\left\{\frac{\sigma}{q}\right\}+\frac{\delta_0 E_s}{B_f q}\{1\} = \left\{I^{f}\right\} \tag{12}$$

Eqn. 12 gives N equations while there are N + 1 unknowns (N normal stresses and 1 uniform translation of the strip). The additional equation is obtained by satisfying the equilibrium of forces at the soil-reinforcement interface as

$$\sum_{i=1}^{N}\left\{\frac{\sigma}{q}\right\} dA \tag{13}$$

Eqns. 12 and 13 are solved by the Gauss Elimination technique for the N values of the normalised normal stresses, $\{\sigma/q\}$, and the normalised rigid body displacement, $\delta_0 E_s/B_f q$

Flexible Strip

If the strip is flexible, the net soil displacements equal the strip deformations, w and is expressed as

$$\left\{\rho_z^f\right\}-\left\{\rho_z^r\right\} = \{w\} \tag{14}$$

The strip is assumed to behave as a beam, the loading on which is the normal stresses mobilised at the interface. The beam equation is

$$E_r I_r \frac{d^2 w}{dx^2} = M \tag{15}$$

where M is the moment and $E_r I_r$ is the flexural rigidity of the beam. The moment of the normal stresses about node i (Fig. 4) is

$$M_i = \sigma_i \frac{dA}{2}\frac{dl}{4} + \sum_{k=i+1}^{N} \delta_k dAx \tag{16}$$

where x is the distance between node i and the centre of the area over which the normal stress σ_k is acting and is the area of the element.

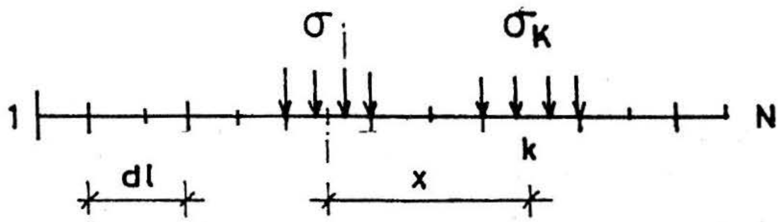

FIGURE 4 : Moment Calculation for Flexible Strip

The vertical displacement of any node i from Eqns. 15 and 16, expressed in the finite difference form is

$$\frac{E_r I_r}{dl^2}[I_b]\{w\} = [I_\sigma]\{\sigma\} \tag{17}$$

where $[I_b]$ is the finite difference coefficient matrix and $[I_\sigma]$ is the moment coefficient matrix.

The boundary conditions for Eqn. 15 are

$$\begin{aligned} &\text{Slope } \frac{dw}{dx} = 0 && \text{At } x = 0 \\ &\text{Moment } \frac{d^2w}{dx^2} = 0 && \text{At } x = L_r \end{aligned} \tag{18}$$

The first boundary condition is applied to Eqn. 15 and the matrix I_b and I_s of size $N-1 \times N$ are obtained. Vectors $\{\sigma\}$ and $\{w\}$ are of size N. The second boundary condition is applied later in terms of the normal stresses.

Substituting for the vector $\{w\}$ from Eqn. 17 into Eqn. 14 one obtains

$$[A]\left\{\frac{\sigma}{q}\right\} = [I_b]\{I^f\} \tag{19}$$

where $[A] = \left[[I_b][I^f] + \frac{(L_r/B_r)^2}{K_B(N-1)^2}[I_\sigma]\right]$ is of size $N-1 \times N$

$K_B = \frac{E_r}{E_s}\frac{I_r}{B_f^4}$ is of size. is defined as the flexibility ratio which takes care of the flexural rigidity of the strip and the modulus of deformation of the soil.

The second boundary condition is now applied in terms of the stresses $\{\sigma\}$. In calculating the moment of forces about node N, stresses mobilised along the whole length of the strip, i.e. $2L_r$ are to be considered. Expressing the moment about node N in terms of the stresses on 2N elements and equating it to zero, one obtains

$$\sum_{i=2}^{N}\frac{\sigma_i}{q}dA + 0.5\left(\frac{\sigma_1}{q}+\frac{\sigma_N}{q}\right)dA = 0 \tag{20}$$

This implies that the force equilibrium is also satisfied. Substituting Eqn. 20 in Eqn. 19 one obtains N equations for the normalised stresses, $\{\sigma/q\}$ which are solved simultaneously. The normalised deformation vector, $\{wE_s/B_fq\}$, of the strip can be obtained from Eqn. 17.

Settlement Reduction

The surface heave profile or the settlement reduction, due to the normal stresses mobilised at the soil-strip interface is arrived at by integrating Mindlin's equation for vertical displacement due to a vertical force within an elastic continuum. The vertical displacement ρ_{zk} of any point k due to a vertical force, $\sigma_j dA$, beneath the surface of a continuum, is

$$\rho_{zk} = \frac{(1+\nu_s)dA}{8\pi E_s(1-\nu_s)}(D)\sigma_j\, dA \tag{21}$$

wherin all the terms are as defined in Eqn. 5. To obtain the vertical displacement of any point k, along the x-axis on the surface due to the normal stress, σ_j, on element j, the following substitutions are made:

$z = 0,$

$c = U_0,$

$R = x^2 + U_0^2$ and

$G_s = E_s/2(1+\nu_s)$

U_0/B_f, length, L_f/B_f

Eqn. 21 then reduces to

$$\rho_{0kj} = \frac{1}{4\pi G_s}\int_A\left(\frac{2(1-\nu_s)}{R}+\frac{U_0^2}{R^3}\right)\sigma_j \, dA \tag{22}$$

Eqn. 22 is rewritten as

$$\rho_{okj}^{r1} = \frac{B_f}{G_s} I_{okj}^{r1}\sigma_j \tag{23}$$

Displacement at point k due to the normal stress σ_j, on the image element j', on the left half of the strip is

$$\rho_{okj}^{r2} = \frac{B_f}{G_s} I_{okj}^{r2}\sigma_j \tag{24}$$

Combining Eqns. 23 and 24, for the influence due to stresses on all elements, the vector of vertical surface displacements, $\{\rho_0^r\}$, is

$$\{\rho_0^r\} = \frac{B_f}{G_s}[I_0^r]\{\sigma\} \tag{25}$$

where $\{I_0^r\}$ is a matrix of influence coefficients for the vertical displacements of points along the surface. The displacements are evaluated at N_f points along the surface. Hence, vector $\{\rho_0^r\}$ is of size N_f and vector $\{\sigma\}$ is of size N while matrix $\{I_0^r\}$ is of size $N_f \times N$ and $I_{0kj}^r = I_{0kj}^{r1} + I_{0kj}^{r2}$

Eqn. 25 is rewritten as

$$\{\rho_o^r\} = \frac{B_f}{G_s}\{I_0\}q \tag{26}$$

where $\{I_0\}$ is a vector of the Settlement Reduction Coefficients (SRC), defined as

$$SRC_k = I_{0k} = \frac{\rho_{0k}^r G_s}{B_f q} \tag{27}$$

Vector $\{I_0\}$ is obtained as

$$\{I_0\} = \left[I_0^r\right]\{\sigma\} \tag{28}$$

Results

For the purpose of integration, the loaded area is divided into elements of size $0.025B_f \times 0.025B_f$. The size of the elements along the strip is $0.1B_f \times 0.1B_f$. The influence coefficient, I_{ij}^r, for the vertical displacement of node i, due to normal stress on element j, is evaluated by dividing the element j into 20 × 20 sub-areas for $\text{abs}(i-j) \leq 2$. Coarser subdivision into 4 × 4 sub-areas was found to be adequate for sub-areas with $\text{abs}(i-j) > 2$. The half-width of the strips $B_r = 0.05B_f$.

A parametric study brings out the effects of depth, U_0/B_f, length, L_f/B_f, the flexibility ratio K_B of the strip reinforcement and the aspect ratio of the loaded area, L_f/B_f on the mobilised normal stresses, σ, the Settlement Reduction Coefficient (SRC) along the surface and the SRC at the centre of the loaded area, I_{sc}. All results are for a Poisson's ratio $\nu_s = 0.3$.

Figure 5 presents the variation of the normalised normal stresses, σ/q, with distance, x/B_f, along the half-length of a rigid strip of length, $L_f/B_f = 2$, for various depths, U_0/B_f, below a square loaded area ($L_f/B_f = 1$).

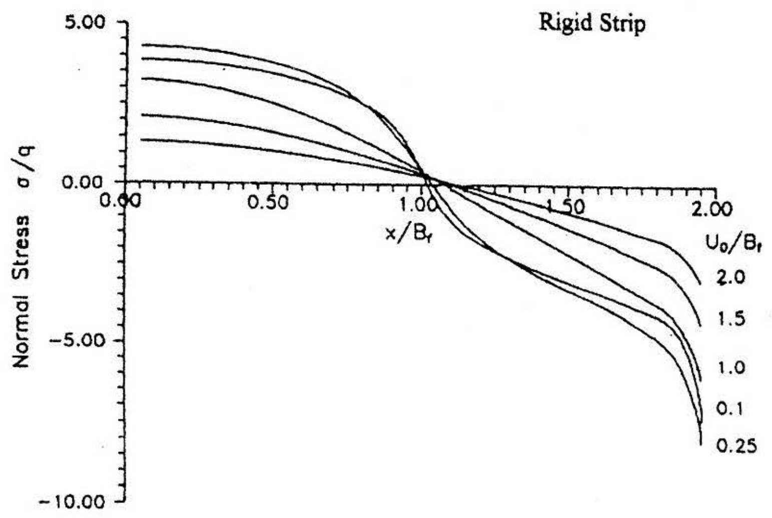

FIGURE 5 : Variation of Normal Stresses with Distance — Effect of Depth of Placement of Strip ($L_r/B_f = 2$, $L_f/B_f = 1$)

A positive stress is one that acts upwards and tends to reduce the surface settlements. Since, for the unreinforced soil, the settlement is maximum for points beneath the centre of the loaded area and relatively large in its vicinity, the mobilised normal stresses are maximum at the centre. Settlement of points at the interface beyond the loaded area is very small. Hence, to equalise settlements for a rigid strip undergoing a uniform displacement, the mobilised normal stresses have to push the strip downward in this region and therefore are negative. It is seen that at distances, x/B_f in the range 1 to 1.15 the stresses change sign. Further, the negative stresses near the edge of the strip increase rapidly and tend to infinity at the edge, which is in consonance with infinite contact stress observed at the edge of rigid footings on elastic continuum. The stresses are the largest for strips at depth, $U_0/B_f = 0.25$. Strips at very shallow depth ($U_0/B_f = 0.1$) show marginally lower stresses due to high interference effect of the normal stresses on displacements of points along the strips. The stresses decrease and tend to be uniform with increase in depth of their placement, as a consequence of relatively uniform settlement of unreinforced soil under the applied load.

The variation of the normalised normal stress, σ/q with the distance x/B_f along the length of a flexible strip of length, $L_f/B_f = 2$ placed below a square loaded area at a depth of $U_0/B_f = 1$ for various values of K_B is depicted in Fig. 6. The stresses for strips with low K_B values ($K_B = 10^{-2}$)

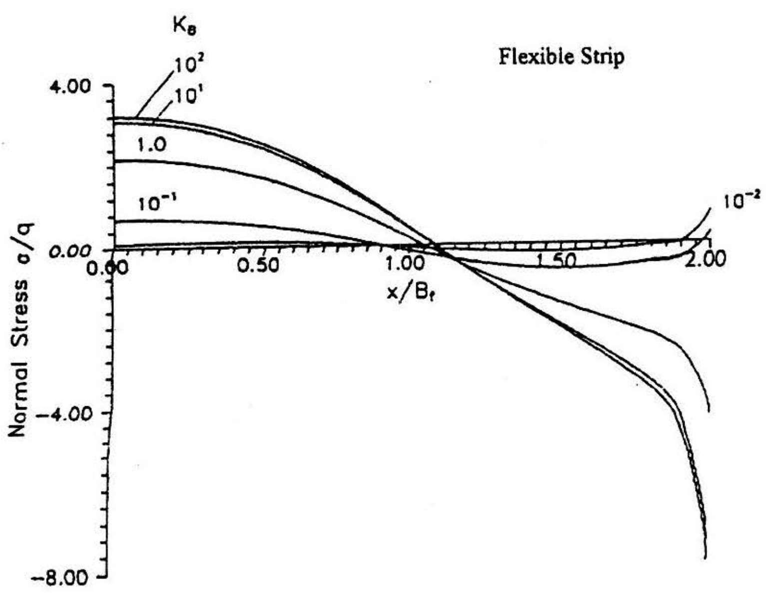

FIGURE 6 : Variation of Normal Stresses with Distance — Effect of Flexibility Ratio of Strip ($L_r/B_f = 2$, $L_f/B_f = 1$, $U_0/B_f = 1$)

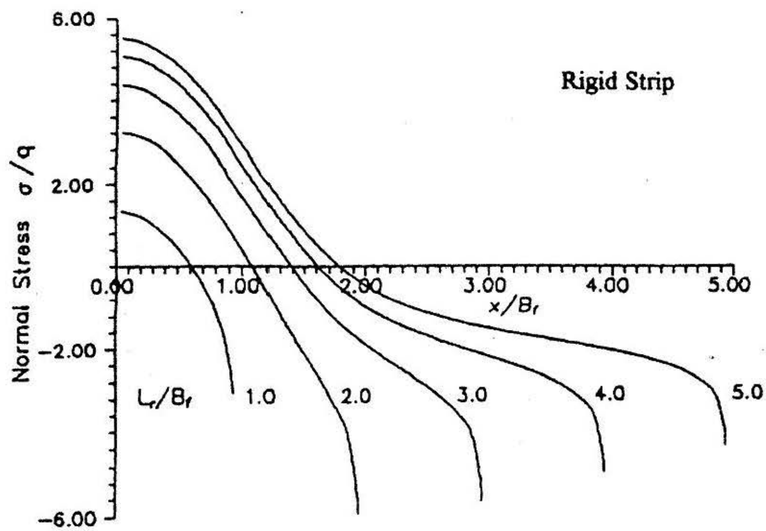

FIGURE 7 : Variation of Normal Stresses with Distance — Effect of Length of Strip ($U_0/B_f = 1$, $L_f/B_f = 1$)

are practically zero. For strips with low K_B values the flexural deflections tend to the vertical displacements of the soil due to the surface loading alone. The normal stresses mobilised in order to counteract the difference in displacements are small. As K_B increases, the stresses increase and tend close to those observed for a rigid strip (Fig. 5). They follow a similar pattern as for rigid strips.

The variation of normal stresses with distance for a rigid strip as affected by its length is depicted in Fig. 7 for U_0/B_f = 1.0 and L_f/B_f = 1.0. For shorter strips (L_f/B_f = 1 and 2), the normal stresses decrease monotonically from a finite positive value and tend to infinity towards the edge of the strip. For longer strips, while the variation of normal stresses with distance is similar to that for shorter strips, the slope of the curve flattens in the portion of the curve where the stresses change sign from positive to negative. This trend is markedly noticed for longer strips (L_f/B_f = 5) possible because the vertical displacements are very small over this portion for the unreinforced soil. The normal stress at the edge tends to infinity at the edge of the strip as observed earlier. The peak normal stress at the centre increases with the length of the strip. For short strips, the relative displacement of points in the soil corresponding to the centre and the edge of the strip is small. Hence, the positive stresses near the center and negative stresses near the edge of the strip required to force the strip to displace uniformly are small. With increasing lengths of the strips this differential displacement increases as displacement of points corresponding to

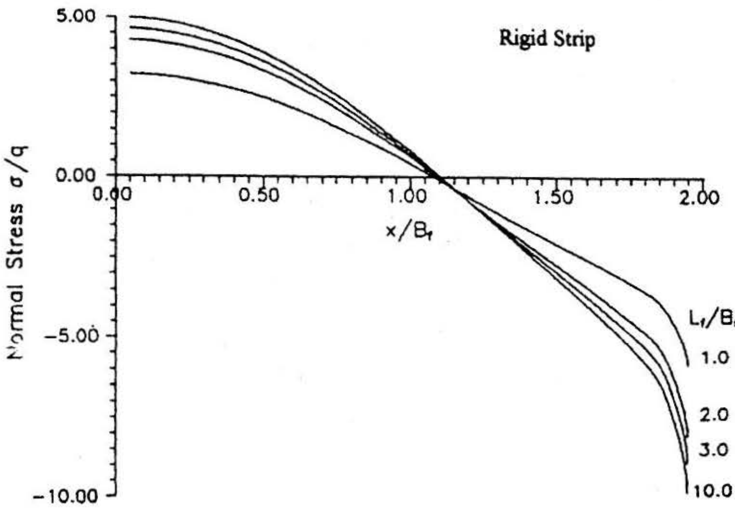

FIGURE 8 : Variation of Normal Stresses with Distance — Effect of Aspect Ratio of Loaded Area ($L_r/B_r = 2$, $U_0/B_r = 1$)

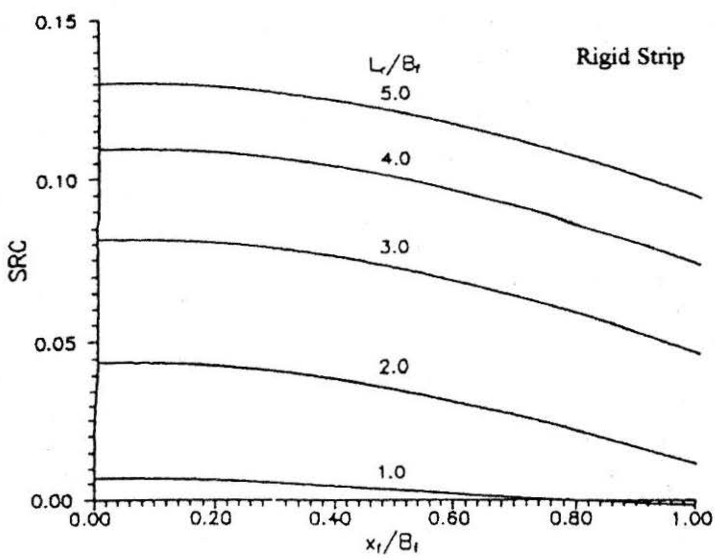

FIGURE 9 : Variation of SRC with Distance along Surface — Effect of Length of Strip ($U_0/B_r = 1$, $L_f/B_r = 1$)

the edge of the strip tend to zero while the central settlement remains the same. Hence, larger positive stresses near the centre and negative stresses near the edge are required to force the strip to displace uniformly. The normalised normal stress at the centre of the strip ($x/B_f = 0$), for $L_f/B_f = 1$ and 5 are 1.3 and 5.5 respectively.

The effect of the shape of the applied load, as defined by the aspect ratio, L_f/B_f , on the normal stress distribution can be noted from Fig. 8 for a rigid strip of length $L_f/B_f = 2$ and placed at a depth $U_0/B_f = 1.0$. The normal stresses are the least for a square loaded area. The stresses increase with increasing aspect ratio, the increase being significant for L_f/B_f increasing from 1 to 2. With further increase in the aspect ratio of the loaded area the increase is marginal because the effect of the applied load on the vertical displacements below the centre for $L_f/B_f > 2$ are small.

Figure 9 depicts the variation of SRC with distance x_f/B_f along the half-width of the loaded area for different lengths, L_f/B_f of a rigid strip placed below a square area at a depth; $U_0/B_f = 1$. A positive SRC indicates heave while a negative one indicates settlement of the surface. The SRC values are maximum at the centre of the loaded area ($x_f/B_f = 0$) and gradually decreases with increase in the distance for all lengths of the strip. It is also noted that SRC values increase with increasing length of the reinforcement strip. The SRC at the centre for $L_f/B_f = 1$ and 5 are 0.007 and 0.13 respectively. The increase in SRC with length of strip is due to the fact that stresses for longer strips are higher than those for shorter ones. The decrease in SRC with increase in x_f/B_f is because the stresses are a maximum at the centre of the strip and decrease with x/B_f.

Figure 10 shows the variation of SRC with x_f/B_f for various U_0/B_f values for a rigid strip of length, $L_f/B_f = 2$, placed below a square area. It is seen that SRC is maximum at the centre of the loaded area and decreases with distance, x_f/B_f . The rate of change of SRC with x_f/B_f is maximum for strips at shallow depths. For strips at greater depths SRC decreases and the curve is almost parallel to the x_f/B_f axis indicating uniform heave of the surface. For strips at shallow depths the effect of the induced normal stresses in reducing surface settlements is high because of the closeness of the reinforcement to the surface. Decrease in stresses with depth result in decrease in SRC with depth of the reinforcement.

The variation of SRC for different aspect ratios, L_f/B_f , of the loaded area for rigid strips of length, $L_f/B_f = 2$, placed at a depth, $U_0/B_f = 1$ is depicted in Fig. 11. It is seen that the increase in SRC for $L_f/B_f = 1$ to 2 is appreciable while with further increase in L_f/B_f the increase in SRC is marginal.

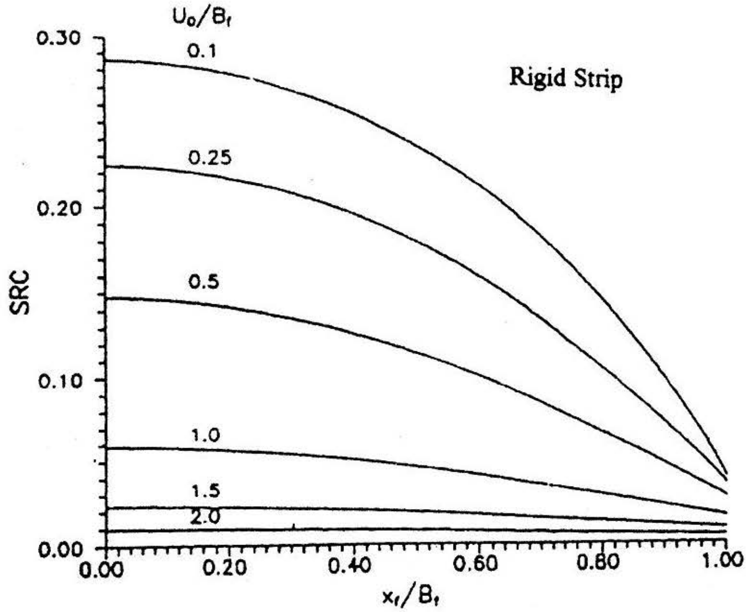

FIGURE 10 : Variation of SRC with Distance along Surface — Effect of Depth of Placement of Strip (L_r/B_r = 2, L_f/B_f = 1)

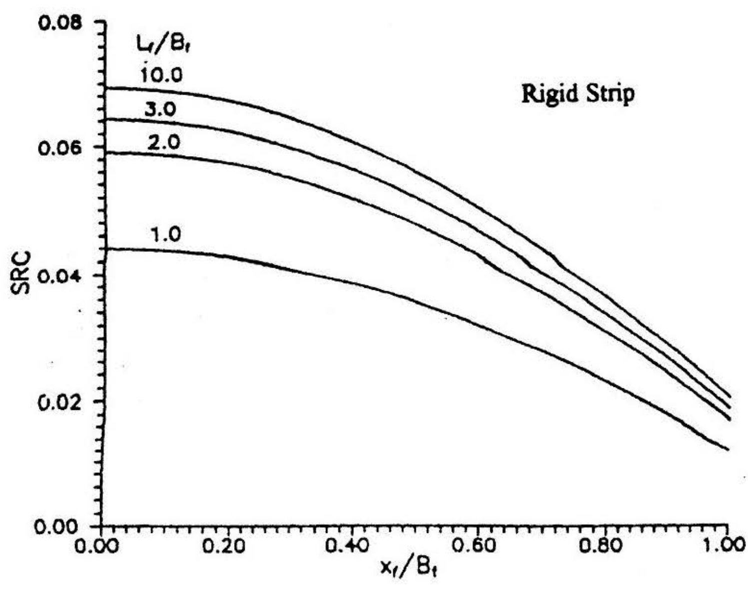

FIGURE 11 : Variation of SRC with Distance along Surface — Effect of Aspect Ratio of Loaded Area (L_r/B_r = 2, U_o/B_f = 1)

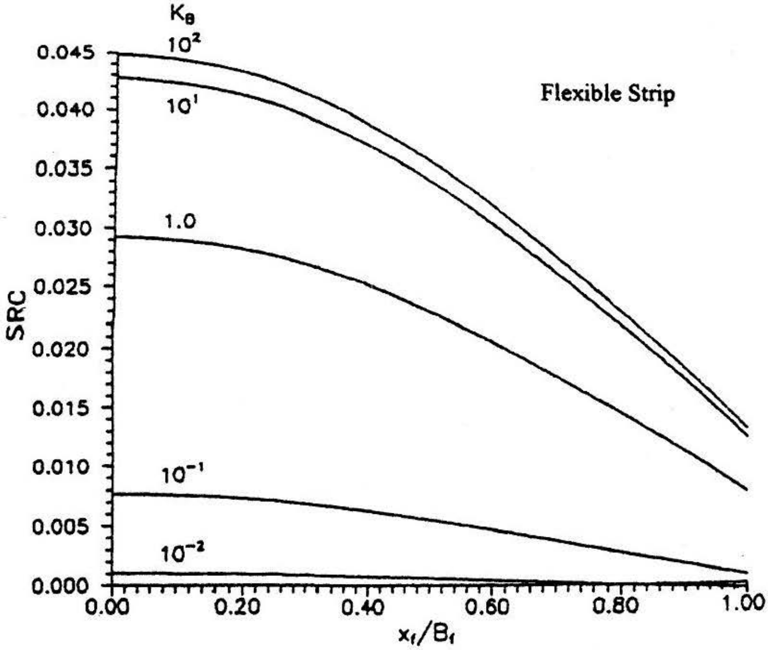

FIGURE 12 : Variation of SRC with Distance along Surface — Effect of Flexibility Ratio of Strip ($L_r/B_r = 2$, $L_f/B_f = 1$, $U_0/B_f = 1$)

The variation of SRC for different flexibility ratios, K_B for a flexible strip of length, $L_f/B_f = 2$ placed below a square area at a depth, $U_0/B_f = 1$ is shown in Fig. 12. The SRC is negligibly small for highly flexible strips (low K_B) because the stresses mobilised at the interface are small. For strips with $K_B = 10^2$, the SRC values coincide with those for a rigid strip with centre and edge showing SRC values of 0.048 and 0.013 respectively. The SRC values at the centre of the strip with $K_B = 1$ is about 0.6 times that of a rigid strip.

The effect of U_0/B_f on the settlement reduction coefficient at the centre of the loaded area, I_{sc}, for different aspect ratios of the loaded area for a rigid strip of length, $L_f/B_f = 2$ is presented in Fig. 13. I_{sc} values decrease with increase in U_0/B_f for all L_f/B_f values confirming the fact that strips at greater depths are ineffective in reducing surface settlements. They increase with increase in L_f/B_f values. The increase is appreciable for L_f/B_f increasing from 1 to 2 whereas the increase is marginal for further increase in L_f/B_f. At a depth, $U_0/B_f = 0.1$, I_{sc} values for $L_f/B_f = 1$ and 10 are 0.245 and 0.31 respectively. The trend shown by the plot is obvious because of the decrease in stresses with increase in depth.

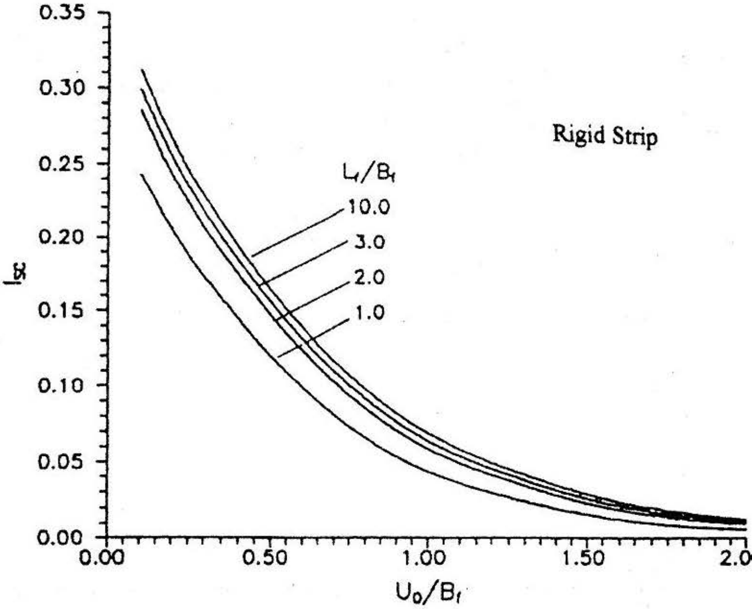

FIGURE 13 : Effect of Depth of Placement of Strip and Aspect Ratio of Loaded Area on I_{sc} (L_r/B_f = 2)

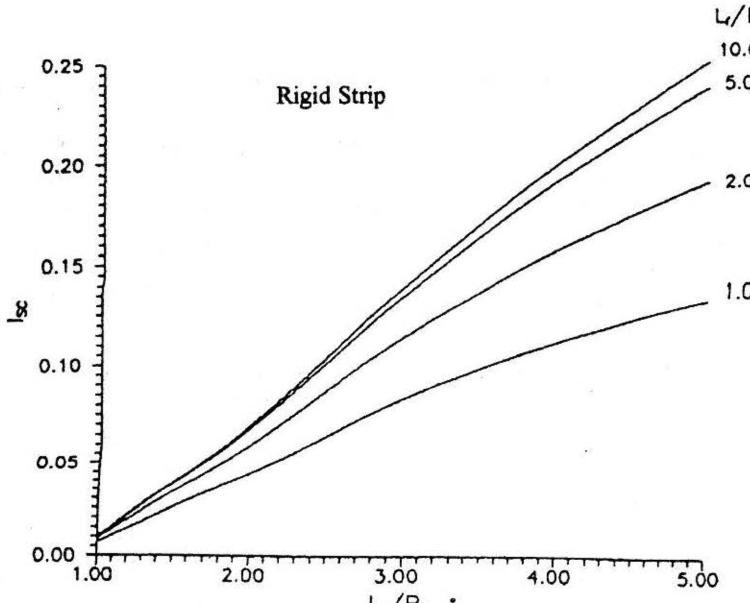

FIGURE 14 : Effect of Length of Strip and Aspect Ratio of Loaded Area on I_{sc} (U_0/B_f = 1)

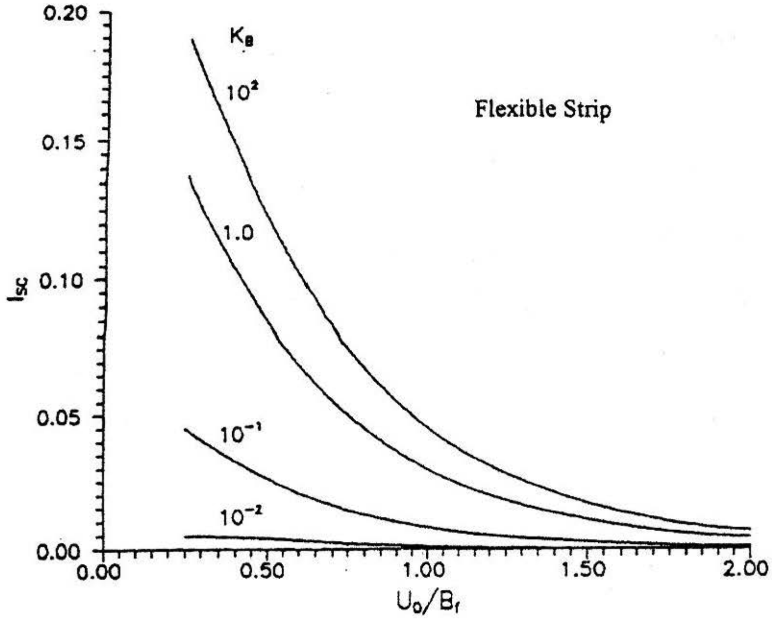

FIGURE 15 : Effect of Depth of Placement of Strip and Length of Strip on Rigid Body Displacement of Strip (L_f/B_f = 1)

Figure 14 depicts the variation of I_{sc} with L_f/B_f for different L_f/B_f values for rigid strips placed at depth $U_0/B_f = 1$. For all L_f/B_f values, the I_{sc} increase with length of the strip. The increase is linear up to $L_f/B_f = 3$ beyond which the curve tends to flatten. This plot shows that below square loaded areas it is sufficient to have strips with length $L_f/B_f = 3$. Longer strips below longer areas are advantageous.

Figure 15 presents the effect of K_B on I_{sc} for different depths, U_0/B_f of a flexible strip of length $L_f/B_f = 2$ placed below a square area. The trend of the curves is similar to that of a rigid strip with the maximum I_{sc} observed at shallow depths. The I_{sc} values decrease rapidly with depth since the stresses mobilised decrease with depth. Highly flexible strips show negligibly small I_{sc} values. Strips with $K_B = 10^2$ show an I_{sc} value of 0.19 at a depth, $U_0/B_f = 0.25$, which is equal to the value for a rigid strip. As the depth increases the effect of K_B on I_{sc} decreases. The I_{sc} value for strips with $K_B = 1$ is 0.135 at a depth, $U_0/B_f = 0.25$ which is about 0.7 times the value for a rigid strip.

The variation of the rigid body displacement, $\delta_0 E_s/B_f q$, of the rigid strip with U_0/B_f for various L_f/B_f values placed below a square loaded area ($L_f/B_f = 1$) is presented in Fig. 16. It is seen that $\delta_0 E_s/B_f q$ decreases

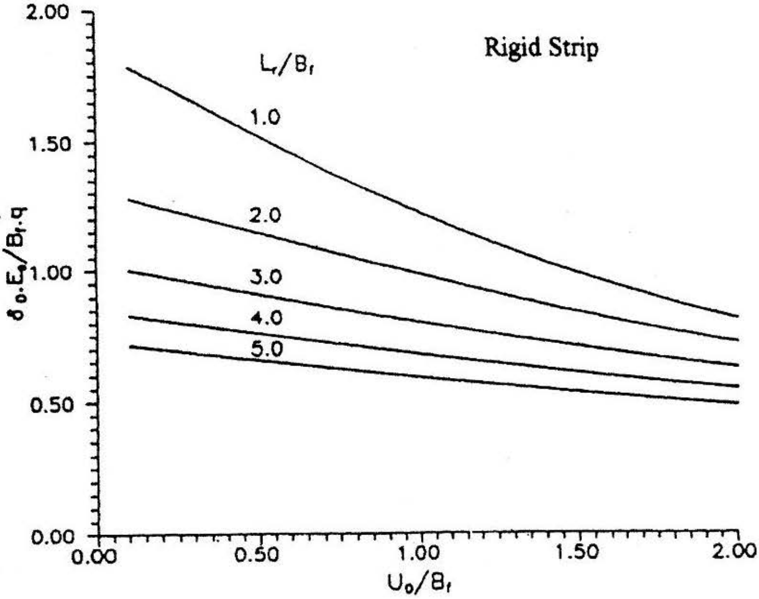

FIGURE 16 : Effect of Depth of Placement and Length of Strip on Rigid Body Displacement of Strip (L_r/B_f = 1)

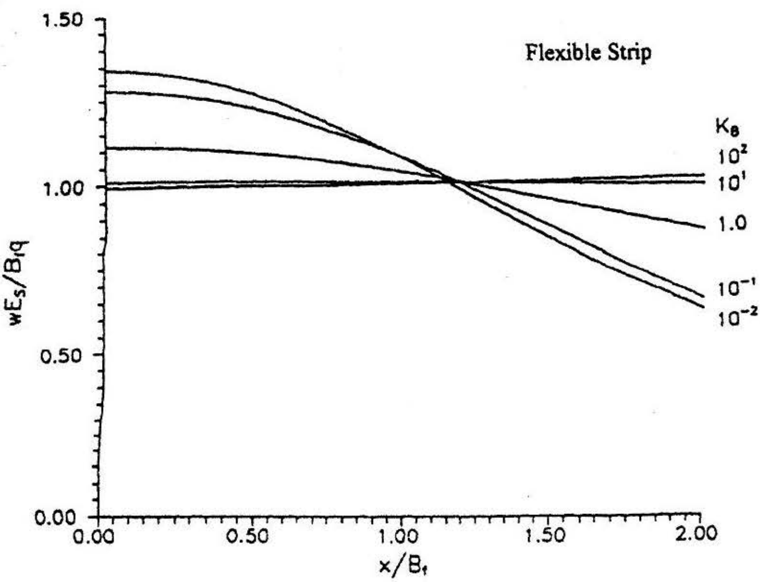

FIGURE 17 : Effect of Flexibility Ratio on Strip Deflection (L_r/B_f = 2, L_f/B_f = 1, U_o/B_f = 1)

with increase in depth, U_0/B_f, and length, L_f/B_f values. The difference between the vertical displacements due to surface loading at the centre and edge of the strip is large for longer strips and small for shorter ones. The uniform displacement value, which a rigid strip maintains, lies in the vicinity of the average value of displacements due to the surface load, which is higher for shorter strips than for a longer one. As a result, $\delta_0 E_s/B_f q$, is maximum for strips with $L_f/B_f = 1$ and minimum for $L_f/B_f = 5$. Further, as U_0/B_f increases, the vertical displacement of points and consequently $\delta_0 E_s/B_f q$ values decreases.

Figure 17 presents the variation of the flexible strip deflections $wE_s/B_f q$, with the distance x/B_f, along the strip for various K_B values, and for strips of length, $L_f/B_f = 2$, placed at a depth, $U_0/B_f = 1$ below a square area. It is seen that for strips with low K_B values ($K_B = 10^{-2}$) the deflections tend to the displacements of the soil due to surface loading. At the centre the deflection, $wE_s/B_f q$ is 1.34 while at the edge it is 0.6. With K_B increasing to 10^2, the deflections equal those for a rigid strip and are equal to the rigid body displacement, $\delta_0 E_s/B_f q$ of 0.99.

Conclusions

An analysis using the elastic continuum approach for a single embedded strip below a uniformly loaded rectangular area is proposed. Satisfying the compatibility of vertical displacements at points along the soil-strip interface and the equilibrium of forces, the net normal stresses mobilised at the strip-soil interface are evaluated. In satisfying the displacement compatibility a rigid strip as well as a flexible one are considered. The resulting uniform translation for a rigid strip and the deflection profile for a flexible strip are evaluated. The reductions in surface settlements due to the mobilised normal stresses are computed.

The results from a parametric study indicate that, for maximum reduction in surface settlements the strip should be placed close to the surface. Below square loaded areas strips of length, $L_f/B_f = 3$ are adequate for maximum settlement reduction. Performance of flexible strips approach that of rigid strips with increase in the flexibility ratio K_B, of the strip which depends on the flexural stiffness and the length of the strip.

References

BROWN, B.S. and POULOS, H.G., (1981) : "Analysis of Foundations on Reinforced Soil", *Proc. X Int. Conf. SMFE*, Stockholm, Vol.3, pp.595-598.

FLOSS, R. and GOLD, G. (1990) : "Use of Finite Element Method for Single Reinforced Two-layered Systems", *Proc. IV Int. Conf. Geotextiles & Geomembranes*, The Hague, Vol.1, pp.248-252.

FRAGASZY, J.P. and LAWTON, E. (1984) : "Bearing Capacity of Reinforced Sand Subgrades", *Jl. of Geotech. Eng. Div.*, ASCE, 110, GT10, pp.1500-1507.

GIROUD, J.P. and NOIRAY, L. (1981) : "Geotextile-reinforced Unpaved Road Design", *Jl. of Geotech. Eng. Div.*, ASCE, 107, GT9, pp.1233-1254.

GUIDO, V.A., BIESIADECKI, G.L. and SULLIVAN, M.J. (1985) : "Bearing Capacity of Geotextile Reinforced Foundation", *Proc. 11th Intl. Conf. Soil Mech. and Found. Engrg.*, San Francisco, 3, pp.1777-1780.

HOULSBY, G.T. and JEWELL, R. (1990) : "Design of Reinforced Unpaved Roads for Small Rut Depths", *Proc. IV Intl. Conf. Geotextiles and Geomembranes*, The Hague, Vol.1, pp.171-176.

HUANG, C.C. and TATSUOKA, F., (1988) : "Prediction of Bearing Capacity on Level Sandy Ground Reinforced with Strip Reinforcement", *Proc. Int. Geotechnical Symp. on Theory and Practice of Earth Reinforcement*, Fukuoka, pp.191-196.

JONES, R.H. and DAWSON, A.R. (1990) : "Reinforced Soil Foundations for Buildings", *Proc. Intl. Reinforced Soil Conf.*, Glasgow, pp.477-478.

MADHAV, M.R., and POOROOSHASB, H.B. (1988) : "A NBW Model for Geosynthatic Reinforced Soils", *Computers and Geotechnics*, 6, pp.277-290.

MADHAV, M.R., and PITCHUMANI, N.K. (1996) : "Numerical Modelling and Analysis of Reinforcement Strip-Soil Interactions", *Proc. 2nd Intl. Conf. in Civil Engg. on Computer Applications, Research and Practice*, Bahrain, pp.579-586.

MIURA, N., SAKAI, A., TAESIRI, Y., MOURI, K.and OHTSUBO, M. (1988) : "Model and Field Tests of Reinforced Pavement on Soft Clay Ground", *Proc. Intl. Geotechnical Symp. on Theory and Practice of Earth Reinforcement*, Fukuoka, pp.227-232.

PITCHUMANI, N.K. and MADHAV, M.R., (1994) : "Soil-Reinforcement Strip Interaction Analysis", *Computer Methods and Advances in Geomechanics*, eds. Siriwardane & Zaman, Balkema, pp.1403-1408.

PITCHUMANI, N.K. and MADHAV, M.R., (1997) : "Analysis of Flexible Reinforcement Strip-Soil Interaction", *Computer Methods and Advances in Geomechanics*, ed. Yuan, Balkema, pp.2349-2354.

SELLMEIJER, J.B. (1990) : "Design of Geotextile Reinforced Roads and Parking Areas", *Proc. IV Intl. Conf. Geotextiles and Geomembranes*, The Hague, Vol.1, pp.177-182.

Notations

B_f = half - width of loaded area

B_r = Half-width of reinforcement strip

c = Depth at which force acts (Mindlin's Problem)

dA = elemental area

E_s = Modulus of deformation of soil

G_s = Shear modulus of soil

I_{sc}	=	Settlement Reduction Coefficient at center of loaded area
K_B	=	Flexibility Ratio for flexible strip
L_f	=	Half-length of loaded area
L_r	=	Half-length of strip reinforcement
n_B	=	number of sub-elements along width of loaded area
n_L	=	number of sub-elements along length of loaded area
N	=	number of elements along half-length of strip
q	=	intensity of loading on surface
SRC	=	Settlement Reduction Coefficient
U_0	=	Depth of placement of strip
w	=	Deflection of flexible strip
x, y, z	=	Cartesian co-ordinates
δ_0	=	Rigid body displacement of rigid strip
ν_s	=	Poisson's ratio of soil
ρ_{zi}	=	Vertical displacement of point i
σ	=	Normal stress mobilised at soil-strip interface